Available online at www.sciencedirect.com
ScienceDirect
International Journal of Fatigue 29 (2007) 261–275
International Journal of Fatigue
www.elsevier.com/locate/ijfatigue

Prediction of fatigue crack growth rate in welded tubular joints using neural network

A. Fathi, A.A. Aghakouchak *

Department of Civil Engineering, Tarbiat Modares University (TMU), Al Ahmed Avenue, P.O. Box 14155-4838, Tehran 14115143, Iran

Received 9 June 2005; received in revised form 26 February 2006; accepted 8 March 2006
Available online 18 May 2006

Abstract

In the past, several methods have been proposed to predict fatigue crack growth rate in tubular joints of offshore structures, however reasonably accurate solution for this problem is still lacking. Dramatic increase in the use of neural neural networks (NN) in material science, specially fatigue area, inspired an investigation on the application of NN in estimating fatigue crack growth rates and stress intensity factors in tubular joints. In this research, four MLP networks are developed to predict weld magnification factor for weld toe cracks in T-butt joints under membrane and bending loading. The training data for these networks are obtained from results of finite element modeling. In addition, two types of neural networks, i.e. MLP and RBF are developed to predict stress intensity modification factors for deepest point of fatigue cracks in tubular T-joint, under axial loading. Experimental data are used to train these networks. The results of above mentioned networks are used to predict fatigue lives of tubular T-joints. The comparison between network results and fatigue lives reported in experiments shows that NN is a successful prediction technique if properly used in this area.

Keywords: Fatigue cracks growth; Offshore tubular joints; Neural network approach; Stress intensity factor

1. Introduction

Welded tubular joints are the most frequently occurring structural detail in jacket type steel offshore platforms. Due to severe cyclic environmental loading experienced by offshore jackets, fatigue has been identified as one of the most important causes affecting the long-term structural integrity. Fatigue damage appears in the form of semi-elliptical surface cracks. In simple tubular joints, these cracks usually initiate from the weld toe and then propagate into the tubular chord wall. This is due to global and local stress concentrations, presence of welding defects and residual stresses introduced by welding process. In surface cracks the crack size is determined by depth (a) and half length (c) as illustrated in Fig. 1.

Fracture mechanics is a powerful tool to estimate fatigue crack growth rate and also residual fatigue life of cracked joints. When offshore platforms are subjected to normal environmental conditions, the global stresses in tubular joints are usually low and plastic zone around cracks tip is small enough to satisfy assumptions of linear elastic fracture mechanics. Hence Paris law is commonly used for predicting the fatigue crack growth rate:

$$\frac{da}{dN} = C(\Delta K)^m, \tag{1}$$

where N is the number of stress cycles, ΔK is stress intensity factor range, C and m are material constants. The difficulty in using Paris law in tubular joints is calculation of the stress intensity factor (K). K may be expressed as a function of total stress range across the wall thickness ($\Delta\sigma$) and crack size (a).

$$\Delta K = Y\Delta\sigma\sqrt{\pi a}, \tag{2}$$

* Corresponding author. Tel.: +98 21 8801001x3322/88754234; fax: +98 21 8005040/88761565.
E-mail address: a_agha@modares.ac.ir (A.A. Aghakouchak).

0142-1123/$ - see front matter © 2006 Elsevier Ltd. All rights reserved.
doi:10.1016/j.ijfatigue.2006.03.002

Nomenclature

a	crack depth
c	crack half surface length
C	crack growth constant in Paris equation
DOB	degree of bending
K	stress intensity factor
L	width of attachment footprint in T-butt joints
m	crack growth exponent in Paris equation
M	crack shape factor in plain plate
MAE	mean absolute error
Mk	weld toe magnification factor
MLP	multi-layer perceptron
NN	neural network
R	correlation factor
RBF	radial basis function
RMS	root mean square error
SC	spread constant in RBF networks
T	chord wall thickness in tubular joints – base plate thickness in T-butt joints
Y	stress intensity modification factor
θ	weld angle
$\Delta\sigma_{HS}$	hot-spot stress range

Subscripts

a	deepest point
b	bending loading
c	crack ends
m	membrane loading

where Y is the stress intensity modification factor which is governed by crack and joint geometry. In the past, several modeling approaches have been attempted for estimating Y factor in tubular joints with various degrees of success. Etube [1] has summarized and categorized these different methods which comprise of experimental measurement, empirical models, numerical models, finite element based models and modified plain plate solutions. Despite the efforts carried out by different researchers, an accurate solution for Y has not yet been obtained. In this research authors try to investigate the capability of neural network to estimate the fatigue crack growth rate and fatigue lives of welded tubular joints. The approach comprises of two main parts:

- Part one: crack depth less than 20% of chord wall thickness

  In early stages of fatigue crack growth process, the deepest point of crack is located in a region which is highly affected by through thickness stress concentrations caused by weld geometry; hence the K factor is primarily affected by weld geometry. T-butt solution is a proper method to estimate K in this stage; hence Y in Eq. (2) may be replaced by $(M \times Mk)$. M is crack shape factor which may be calculated by well validated plain plate solutions and modified by weld magnification factor (Mk) to consider weldment geometry effects in calculating K. Four neural networks are developed to estimate Mk at deepest point and crack ends in T-butt joints under membrane and bending loading. These Mk factors can be used to modify shape factors which are calculated by Newman–Raju equations [2].
- Part two: crack depth more than 20% of chard wall

  When the fatigue cracks grow larger and a/T is greater than 0.2, the deepest point of crack is in such a zone that weld geometry effects can be neglected in calculating K factor, especially in deepest point, i.e. $Mk = 1.0$. So crack growth process may be considered to be a function of crack geometry, joint geometry and loading mode. These parameters determine the stress distribution at tubular intersection and load shedding mechanism, which are the most effective parameters in estimation of K factor and crack growth regime. For this part, two types of neural networks are designed and trained to predict the Y factor in deepest point of fatigue cracks in tubular T-joints under axial loading.

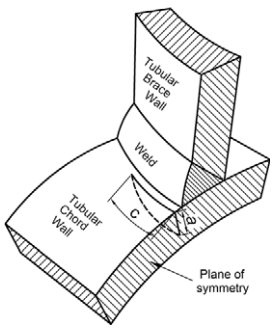

Fig. 1. Semi-elliptical surface crack in a tubular joint.

2. Neural networks

Neural networks (NN) are considered as artificial intelligence modeling techniques. They have a highly interconnected structure similar to brain cells of human neural networks and consist of the large number of simple processing elements called neurons, which are arranged in different layers in the network; an input layer, an output layer and one or more hidden layers. The input neurons receive and process the input signals and send an output signal to other neurons in the network. Each neuron can be connected to other neurons in next layer. Each neuron has a transfer function, which can be continuous, linear or non-linear function. The signal passing through a neuron is transformed by weights (which modify the inputs) and

by the transfer functions and then reaches the following neurons. Modifying the weights of neurons in the network changes the output.

One of the well-known advantages of NN is that the NN has the ability to learn from the sample set, which is called training set, in a supervised or unsupervised learning process. Once the architecture of network is defined, then through learning process, weights are calculated so as to present the desire output. Several different architecture and topologies have been proposed for NN. They differ in terms of architecture, learning process and training strategies. A linear model can be represented adequately by single layer network while a non-linear model generally requires a multiple layer network [3]. Two types of NN, which are used in this work, are briefly reviewed here.

2.1. Multi-layer perceptron (MLP) network

MLP is a feed forward network with one or more hidden layers in which each neuron is connected to neurons of the next layer. MLP is the most popular type of neural network. The basic unit of the network is a perceptron. This is a computation unit, which produces its output by taking a linear combination of the input signals and transforming it by a transfer function. The transfer function used in the hidden layer is usually nonlinear but the transfer function in the output layer can be either nonlinear or linear [3].

Each input unit of the input layer receives input signal (x_i) and broadcasts this signal to all units in the hidden layer. Each hidden unit (y_j) sums its weighted input signal and applies its transfer function to compute output signal.

$$y_j = f\left(\sum_{i=1} w_{ij}x_i + b_i\right), \tag{3}$$

where w_{ij} is the weight from the input unit (x_i) to the hidden unit (y_j) and b_i is the bias. The output signal of the hidden unit (y_j) is sent to all units in the next hidden or output layer. Each output unit (o_k) sums its weighted input signal and applies its transfer function to compute its output signal.

$$o_k = f\left(\sum_{j=1} w_{jk}x_j + b_i\right), \tag{4}$$

where w_{jk} is the weight from the hidden unit (y_j) to the output unit (o_k). The transfer function which is widely used in MLPs is a logistic sigmoid function defined as:

$$f(x) = \frac{1}{1+\exp(-x)}. \tag{5}$$

Back propagation (BP), which is one of the most famous training algorithms for multilayer perceptions, is a gradient descent technique to minimize the error for particular training pattern. Although BP training algorithm has some drawbacks, this method is being used because it is simple and reliable. Training algorithm is an iterative gradient descent algorithm, designed to minimize the sum of square error (E) which is averaged over all patterns and is calculated as follows

$$E = \frac{1}{2}\sum_{i=1}^{P}\sum_{k=1}^{K}(d_{pk} - o_{pk})^2, \tag{6}$$

where d_{pk} is the desired or actual output, o_{pk} is the predicted output for the pkth pattern. During training, an NN is presented with the data for hundreds of times, which is referred to as cycles. After each cycle, the error between the NN output (predicted) and desired values are propagated backward to adjust the weight in a manner mathematically guaranteed to converge. Adjustments of the weights (Δw_{ij}) can be calculated as

$$\Delta w_{ij} = -\alpha\frac{\partial E}{\partial w_{ij}} + \beta\Delta w_{ij}(s-1), \tag{7}$$

where a is the learning rate, β is the momentum coefficient and s is the current step. Detailed description of the mathematical formulation of the BP algorithm has been covered in literature extensively [3]. Training is the act of continuously adjusting the connection weights until they reach unique values that allow the network to produce outputs that are close enough to the actual desired outputs. The accuracy of the developed model, therefore, depends on these weights. Once optimum weights are reached, the weights and biased values encode the network's state of knowledge. MLP networks maintain a high level of research interest due to their ability to map any function to an arbitrary degree of accuracy. MLP networks have been applied to many diverse areas such as pattern recognition, time series prediction, signal processing, control and a variety of mathematical applications [3].

2.2. Radial basis function (RBF) network

The RBF network consists of one hidden layer. Each unit in the hidden layer, called RBF unit, represents a single radial basis function, with associated center position and width. Each neuron on the hidden layer employs a radial basis function as nonlinear transfer function to operate on the input data. The most often used RBF is Gaussian function that is characterized by a center (c_j) and width (r_j). RBF functions by measuring the Euclidean distance between input vector (x) and the radial basis function center (c_j) and performs the nonlinear transformation with RBF in the hidden layer as given in below:

$$h_j(x) = \exp(-\|x - c_j\|^2/r_j^2). \tag{8}$$

In which, h_j is the notation for the output of the jth RBF unit. For the jth RBF, c_j and r_j are the center and width, respectively. The operation of the output layer is linear, which is given in Eq. (9)

$$y_k(x) = \sum_{j=1}^{n_h} w_{kj} h_j(x) + b_k, \tag{9}$$

where y_k is the kth output unit for the input vector (x), w_{kj} the weight connection between the kth output unit and the jth hidden layer unit and b_k the bias.

Training the RBF networks consists of two separate stages. In the first stage, the weights between the input and hidden layers are determined given a specific number of pattern units (i.e. clusters). For this, an unsupervised, clustering algorithm called the k-means algorithm is typically used. In this algorithm, k training input patterns are first sampled from n training input patterns. These k vectors are regarded as the initial center vectors for the k clusters. For each of the remaining $(n-k)$ training input patterns, Euclidean distance to each center vector is calculated. A training input pattern is then classified into a particular cluster, to which the Euclidean distance is minimized. The center vector of this cluster chosen is subsequently updated by calculating the mean of the center vector and the training input pattern classified. In this way, other training patterns are classified while continuously updating k center vectors. The first stage is completed by assigning each of all training input patterns to a specific cluster by comparing Euclidean distances with respect to the final updates of the center vectors [4].

As the second training factor, the widths of radial basis functions are frequently optimized in a heuristic way. The other weights between the hidden and output layers are determined in a supervised or deterministic way. The latter deterministic way is typically determined by the least mean square algorithm and the resulting weight (W) matrix between the pattern and output layers is simply expressed as

$$W = (O^T O)^{-1} O^T T, \tag{10}$$

where O and T represent the output matrix of the hidden layer and target matrix, respectively. The RBF networks with deterministic training way for output layer are called exact RBF networks.

The RBF has attracted a lot of interest since its conception. RBF networks approximate nonlinear systems with outputs that are linear combinations of the network weights. Therefore, it is relatively easier to derive the learning algorithm of the weights with a higher rate of convergence in the RBF networks than in the MLP structure for some problems. Besides, it has been acknowledged that in many problems, approximation properties of RBF networks are advantageous as compared to other methods including MLP networks [5].

3. Evaluating the Y factor in tubular T-joints using NN

3.1. Experimental training data

Experimental Y factor data used for training and testing the networks are obtained from large scale fatigue tests on six tubular T-joints. These tests are carried out by Myers [6] in NDE center of University College London. Fig. 2 shows the geometry parameters of joints and applied loading mode. The fatigue data have been gathered by applying constant amplitude axial load to the brace of joints. Two joints have been tested in air and other four ones in seawater environment with cathodic protection. Cathodic protection was used to reduce the rate of corrosion to a level that would allow the structure to attain its design life [1], so the same material constants (C,m) can be used for the joints in sea water and the joints in air. Table 1 shows the applied stress ranges and environmental condition of each joint. The alternative current potential drop (ACPD) method has been used to measure crack sizes during crack growth period.

Determination of experimental Y factor relies on the use of Paris crack growth law. Based on this assumption, Y factor is obtained from Eq. (11):

$$Y = \left(\frac{1}{\Delta\sigma_{HS}\sqrt{\pi a}}\right)\left(\frac{da/dN}{C}\right)^{1/m}. \tag{11}$$

The accuracy of experimental Y factors depends on the material constants, C and m used in Paris equation. The C and m values recommended by NDE center [7] for the experiments are 2.72×10^{-12} and 3.532, respectively. After calculating the Y factor at deepest point of cracks in various stages of experiment, the data related to crack sizes from $a/T > 0.2$ up to $a/T = 1$ are selected. This is because when $a/T < 0.2$, the crack growth process is highly affected by weld geometry. So 177 patterns are obtained which provide Y factors at deepest point of cracks with correspond-

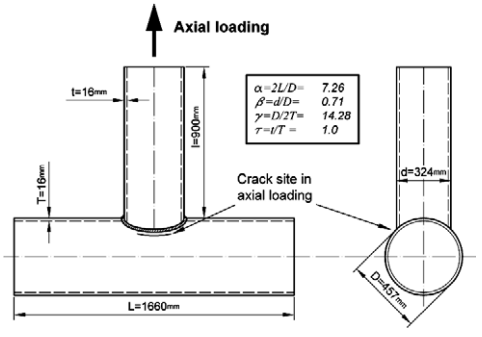

Fig. 2. Nominal specimen dimensions and loading mode for six T-joints.

Table 1
Applied stress ranges and environmental condition for six T-joints [5]

Test number	$\Delta\sigma_{HS}$ (MPa)	Environment
T1	400	(Air)
T2	300	(Air)
T3	225	(−1000 mV)
T4	225	(−800 mV)
T5	300	(−1000 mV)
T6	300	(−800 mV)

ing a/T and a/c. The resulting Y factors at deepest point of cracks (Y_a) versus a/T and a/c are shown in Fig. 3.

3.2. Neural network modeling

Several research works have been carried out recently on the use of NN in fatigue area [8–11], most of them used MLP networks to predict desire outputs. However, RBF has been described as potential alternative approach to replace MLP networks in many research areas because this network offers some advantages such as robustness to noisy data, compared with MLP [12]. In Sections 2.1 and 2.2, the advantages of MLP and RBF networks were discussed. In the following paragraph some differences between these two types of network are briefly described.

An RBF is trained when two sets of parameters (the centers and the widths) in the hidden layer and a set of weights in the output layer are adjusted. As the adjustment of the output layer is simple, RBF network has a guaranteed learning procedure for convergence. However, in back-propagation MLP, the parameters of transfer functions both in hidden and output layers should be adjusted by using the logistic sigmoid transfer functions and generally it is time-consuming. The RBF system lacks all the attributes that go with the natural-inspired methods, such as NN and genetic algorithm. All natural-inspired methods have in common: (a) any form of randomness influencing the outcome of the procedure (sample order, initialization of weights, etc.), (b) similarity to some natural phenomenon (functioning of biological neuron, survival of the fittest, etc.), and (c) an iterative learning procedure, with the number of iteration steps influencing the results. RBF networks has none of these features and can be solved straightly [12].

Furthermore, there are a number of significant architectural differences between RBFs and MLPs [13]:

- The RBF has one hidden layer while the MLP can have several.
- The hidden and output layer nodes of the RBF are different while the MLP nodes are usually the same throughout.
- RBFs are locally tuned while MLPs construct a global function approximation.

Considering all the differences and advantages/disadvantages of each network, both types have been used in this research to ensure appropriate handling of the noises which exist in experimental database. These noises exist due to inaccuracies in load monitoring and crack dimension measurement techniques as well as human errors, etc.

The networks are designed to evaluate the Y factor at deepest point of fatigue cracks in tubular T-joints under axial loading when ($0.2 < a/T < 1.0$). The required input data for this prediction are a/T and a/c. Initially the 177 available patterns are divided into two parts; one part for training the networks and the other one for testing the efficiency of the trained networks. In dividing the patterns, the ones, which include the maximum and minimum values, are placed in training set; because the NN cannot extrapolate beyond the limits of training set values. Based on above 118 patterns are allocated to training and the rest of them, i.e. 59 patterns, are placed in testing set. The training set is selected in the same manner from each one of six joints data. Subsequently the Y factors for all patterns are normalized between 0 and 1.0, because the logistic sigmoid transfer function, which is used in MLP network, gives the values between 0 and 1.0.

For the MLP networks the logistic sigmoid transfer function is assigned to all neurons in different layers and BP algorithm is selected for training. For RBF networks, the Gaussian transfer function is assigned to neurons in hidden layer and linear function is used for output layer.

Several types of NN architectures are possible using various number and arrangement of layers and neurons. The procedure for selecting the best network is a trial and error one; but the number of neurons in output layer is predefined by the problem, i.e. they are equal to number of target parameters. For this problem the required number of output neuron is one. MLP networks with one or two hidden layers and different number of neurons in layers were designed, trained and tested. Fig. 4 shows the root mean square (RMS) error for results of networks for training and testing sets. As the figures show, the most accurate

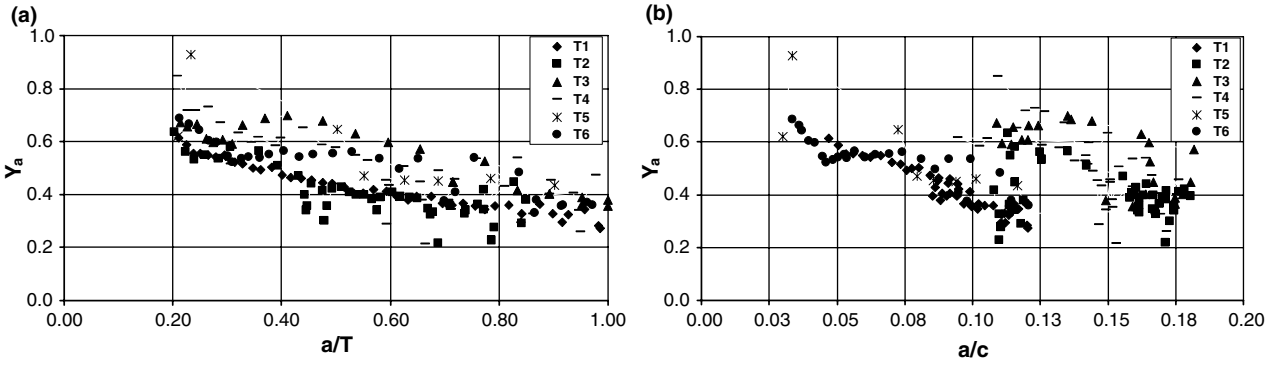

Fig. 3. Y at crack deepest point versus a/T and a/c for six joints.

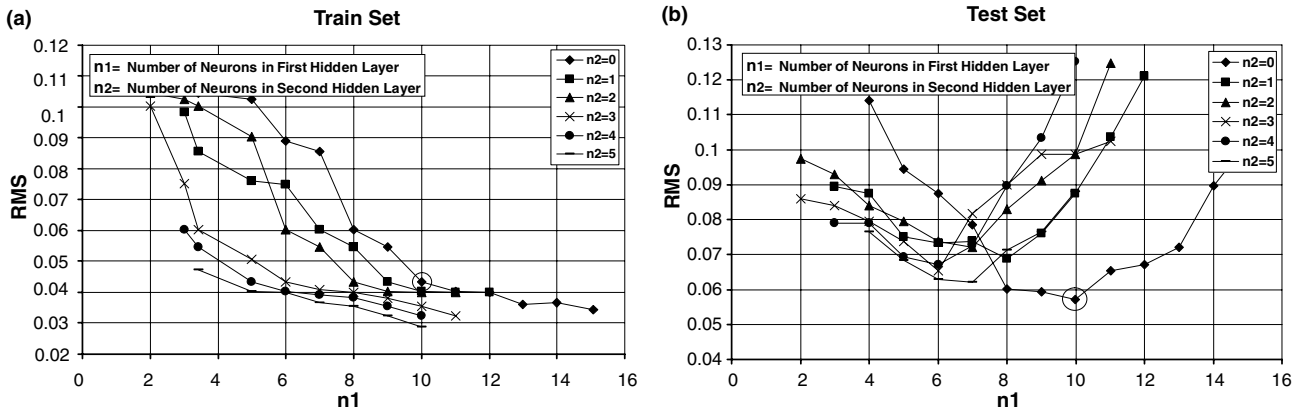

Fig. 4. RMS for different MLP architecture – train and test sets.

results belong to the two-layer MLP network, which has 10 neurons in hidden layer. In Fig. 5, the results of Y factors predicted by this MLP network versus experimental values and the corresponding *trendlines* are shown.

For the RBF network the exact type of RBF networks is used. In the exact RBF networks the number of hidden nodes are equal to the number of nodes in the hidden layer. In this way, the only adjustable parameter is spread constant (SC). SC is in relation with the spread of radial basis functions in the network. Each bias in the first layer is set to 0.8326/SC. This gives radial basis functions that cross 0.5 at weighted inputs of ±SPREAD. This determines the width of an area in the input space to which each neuron responds. If SC is 4, then each neuron in hidden layer will respond with 0.5 or more to any input vector within a Euclidean distance of 4 from their RBF centers. SC should be large enough that neurons respond strongly to overlapping regions of the input space.

The only condition which needs to be met is to make sure that SC is large enough so that the active input regions of the neurons in hidden layer overlap enough, hence neurons always have fairly large outputs at any given moment. This makes the network function smoother and results in better generalization for new input vectors occurring between input vectors used in the design. (However, SC should not be so large that each neuron is effectively responding in the same, large, area of the input space [5].)

In Fig. 6 the mean absolute error (MAE) of the results of networks with different value of SC are shown. It is

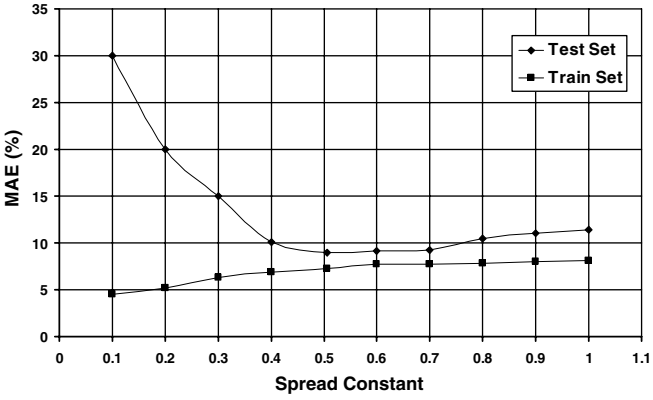

Fig. 6. MAE for RBF networks with different SC.

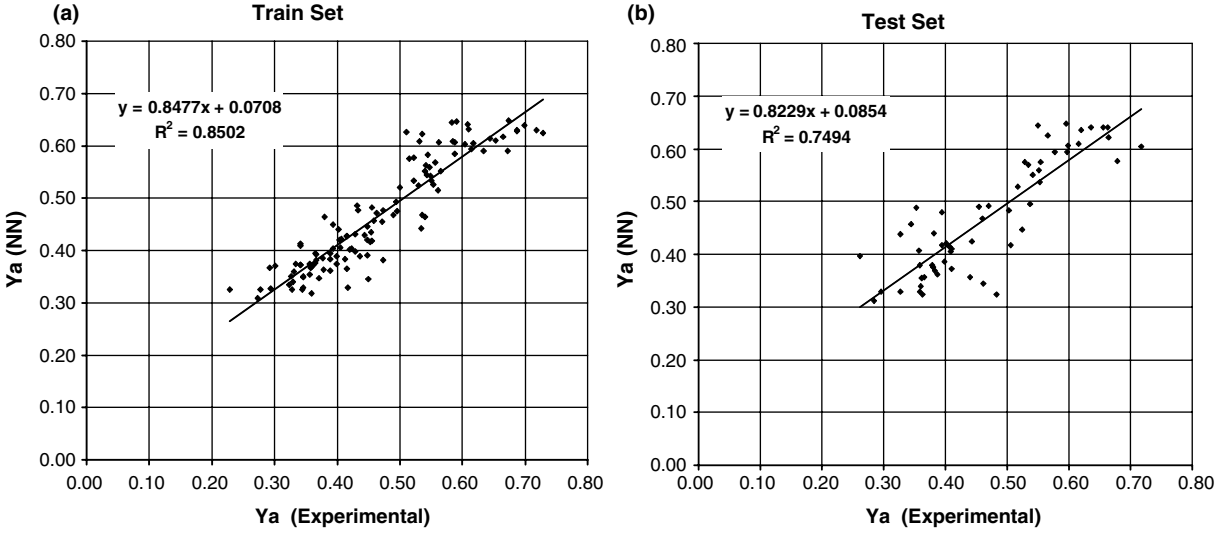

Fig. 5. Y values predicted by MLP versus experimental values – train and test sets.

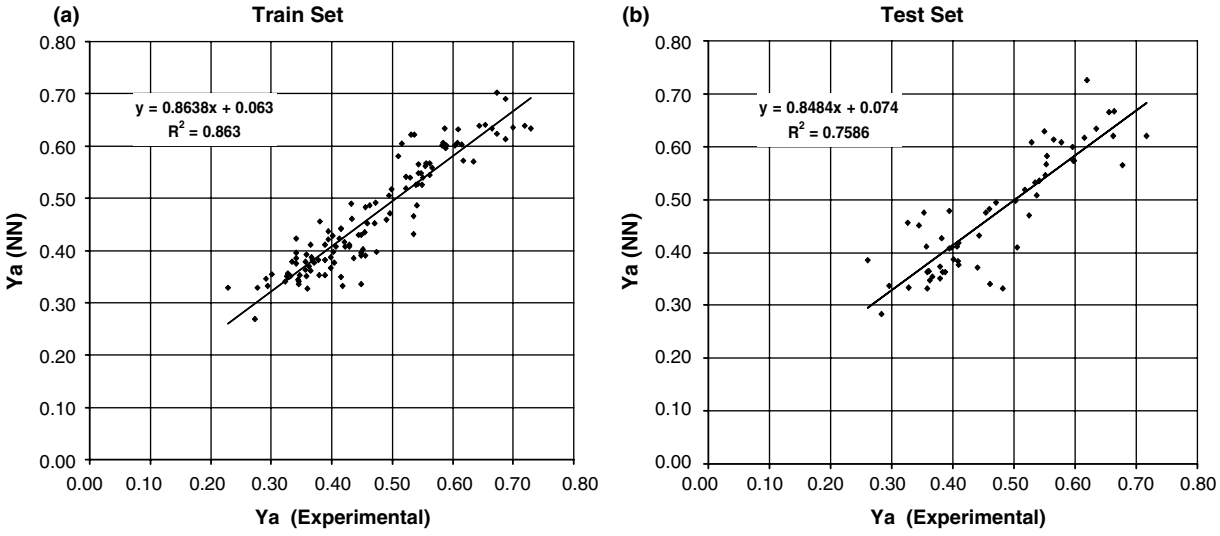

Fig. 7. Y values predicted by RBF versus experimental values – train and test sets.

evident that the best RBF network is the one, which has a SC equal to 0.505. In Fig. 7, the results of predicted Y factor by this RBF network are shown versus experimental values. Different indicators of errors for the optimal RBF and MLP networks are shown in Table 2, which illustrates that the results of the RBF network have better agreement with experimental Y factors.

Table 2
MLP and RBF characteristics for Y prediction

Network characteristics	MLP network for predicting Y	RBF network for predicting Y
Network architecture		
Required input data	a/T, a/c	
Number of neurons in output layer	1	1
Transfer function in output layer	Logistic sigmoid	Gaussian
Number of neurons in 1st hidden layer	10	118
Transfer function in 1st hidden layer	Logistic sigmoid	Linear
Train parameters		
Learning algorithm	Back propagation	k-mean
Learning rate	0.4	–
Momentum coefficient	0.5	–
Number of learning cycles	300	100
Number of learning patterns	118	118
Maximum error (%)	23.0577	25.3770
Minimum error (%)	−42.6161	−44.3974
RMS	0.0434	0.0415
R	0.9221	0.9290
MAE (%)	7.5146	7.2341
Test parameters		
Number of testing patterns	59	59
Maximum error (%)	32.7939	31.3851
Minimum error (%)	−51.6138	−47.7918
RMS	0.0572	0.0566
R	0.8657	0.8710
MAE (%)	9.4148	8.9599

Another criterion, which is frequently used to determine the efficiency of trained NN, is frequency of error. Frequency of error demonstrates the prediction error in each percent of database. Fig. 8 shows the comparison of error frequency between the most efficient RBF and the MLP networks in train and test sets. As shown in this figure, the trained networks can predict Y factor with about 5% absolute error, in 80% of testing data set.

3.3. Comparisons with other methods

The results of the best MLP and RBF networks for estimating the Y factor for complete set of data from six T-joints are compared with the results of some previous models namely:

- Average stress model (AVS) proposed by Dover et al. [14].
- Modified average stress model (MAVS) proposed by Austin JA [15].
- Two phase model (TPM) proposed by Kam JC [16].
- Newman–Raju formula [2] in conjunction with linear moment release model (NR-WLMR) proposed by Aghakouchak et al. [17].
- The new empirical model for Y joints proposed by Etube et al.[1] [18].

In Fig. 9a the *correlation factors* $(R)^2$ of Y factors from different methods and experimental ones are shown for entire data of six joints. In Fig. 9b, the RMS in predicting the Y factor for each method are illustrated. These Figures

[1] Etube et.al. [11] suggested that their new model may be used for other joints with caution.
[2] $R_{x,y} = \frac{Cov(X,Y)}{\sigma_x \cdot \sigma_y}$.

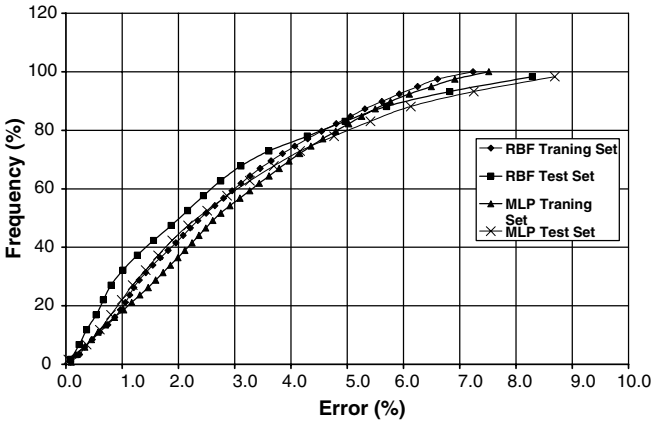

Fig. 8. Frequency of error for MLP and RBF networks.

show that the developed neural networks can evaluate the Y factor more accurately compared to other methods.

4. Evaluating the *Mk* using neural network

The equations proposed by Newman and Raju [2] for stress intensity factors for surface cracks in plates, are often used in Fracture Mechanics analysis of cracks in tubular joints. This method should be used in conjunction with a structural modeling method to consider the boundary conditions and geometrical differences between plain plates and tubular joints. Some adapting models were proposed in this regard by Aghakouchak [17], Myers [6] and Monahan [19]. Each of these adapting methods tries to address some shortcomings of plain plate solutions such as the effects of load shedding, intersection stress distribution and weld magnification on K factors in tubular joints.

T-butt solution is a method to estimate K factors for cracks in the plain base plate with a perpendicular welded attachment. This method estimates the weld geometry effects on crack growth rate by calculating weld magnification factor (Mk). Hence the T-butt solution can be categorized as an adapted plain plate solution in which the weldment effects on plain plate is considered. This method has the inherent properties similar to plain plate solution.

The most remarkable feature of T-butt solution is the capability of this method to assess the fatigue cracks in tubular joints when the crack is in the earlier stages of growth. Cheaitant et al. [20] recommended T-butt solution as the best method to evaluate stress intensity factor in tubular joints when $0 < a/T < 0.2$ because for cracks of this size:

- The most affecting parameter on crack growth process is weldment geometry; and T-butt solution is an appropriate method to consider this.
- The crack dimension is relatively small compared to joint dimension. Hence using the hot spot stress instead of stress distribution at the intersection does not make any significant differences for crack ends.
- The global stiffness of joint is not considerably different from untracked joint. So in deepest point of crack the effects of load shedding can be neglected and crack growth is almost independent of joint geometry and loading mode.

4.1. Finite element based training data

Bowness and Lee [21] have published invaluable parametric equations for estimating Mk in deepest point and ends of weld toe cracks in T-butt joints, under membrane and bending loading. They have generated comprehensive database from finite element modeling for different crack and weld geometry. Fig. 10 shows the T-butt joint and related geometrical parameters of weld and crack. As shown in the figure, a and c are crack depth and half length, respectively, L is attachment footprint and θ is weld angle. In this research the data for $0.005 \leqslant a/T \leqslant 0.2$ were extracted from the database published by Lee and Bowness [22]. These data comprise 399 pattern of different value of a/T, a/c, L/T and θ for sharp welds in T-butt joints. Table 3 shows the variation matrix of these parameters. There are four output parameters for each input pattern:

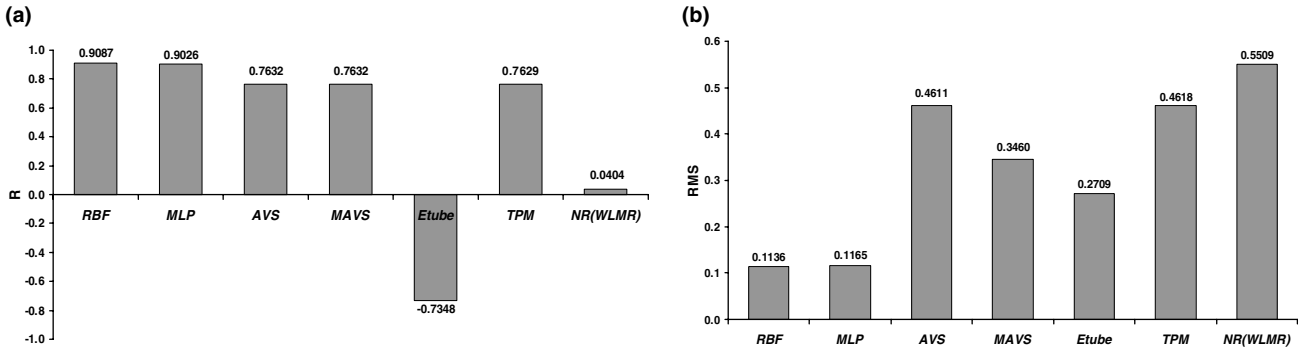

Fig. 9. Correlation factor and RMS in predicting Y by different solutions.

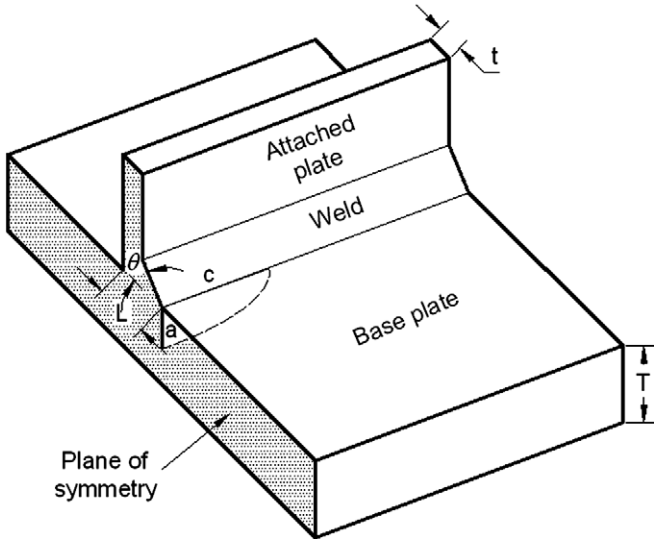

Fig. 10. Geometrical parameters for T-butt joints.

Table 3
Variation of parameters of input patterns – T-butt method

Input parameter	Variation
a/T	0.005, 0.01, 0.02, 0.04, 0.07, 0.1 and 0.2
a/c	0.1, 0.2, 0.4 and 1.0
θ	30°, 45°, 60° and 75°
L/T	0.5, 1.25, 2.0 and 2.75

Mk_{ma}: weld magnification factor at deepest point of crack under membrane loading.
Mk_{ba}: weld magnification factor at deepest point of crack under bending loading.
Mk_{mc}: weld magnification factor at crack ends under membrane loading.
Mk_{bc}: weld magnification factor at crack ends under bending loading.

4.2. Designing and training the networks

Principals and procedures used to develop NN in this section are the same as the ones used in previous section for Y factors in tubular T-joints. Four MLP network are designed in order to predict Mk_{ma}, Mk_{ba}, Mk_{mc} and Mk_{bc} when $0.005 \leqslant a/T \leqslant 0.2$. Then the stress intensity factor can be calculated using the flowing equation:

$$\Delta K_{\text{tubular joint}} = [M_m Mk_m(1 - \text{DOB}) + M_b Mk_b \text{DOB}]\Delta\sigma_{HS}\sqrt{(\pi a)}, \quad (12)$$

where DOB is the degree of bending, $\Delta\sigma_{HS}$ is hot-spot stress range in the weld toe on the reference brace of the joint (weld toe stress concentration should not be considered in calculating the $\Delta\sigma_{HS}$) and M_m and M_b are the plain

Table 4
MLP characteristics for Mk predictions

Network characteristics	MLP network for predicting Mk_{ma}	MLP network for predicting Mk_{ba}	MLP network for predicting Mk_{mc}	MLP network for predicting Mk_{bc}
Network architecture				
Required input data	a/T, a/c, L/T and θ			
Number of neurons in output layer	1	1	1	1
Transfer function in output layer	Logistic sigmoid	Logistic sigmoid	Logistic sigmoid	Logistic sigmoid
Number of neurons in 1st hidden layer	9	15	12	12
Transfer function in 1st hidden layer	Logistic sigmoid	Logistic sigmoid	Logistic sigmoid	Logistic sigmoid
Number of neurons in 2nd hidden layer	7	5	12	12
Transfer function in 2nd hidden layer	Logistic sigmoid	Logistic sigmoid	Logistic sigmoid	Logistic sigmoid
Number of neurons in 3rd hidden layer	–	–	7	7
Transfer function in 3rd hidden layer	–	–	Logistic sigmoid	Logistic sigmoid
Network training				
Learning algorithm	Back propagation			
Learning rate	0.1	0.1	0.1	0.1
Momentum coefficient	0.1	0.1	0.1	0.1
Number of learning cycles	1500	2750	375	450
Number of learning patterns	270	270	270	270
Maximum error (%)	0.8408	0.6762	1.6184	3.3909
Minimum error (%)	−0.8206	−0.5244	−4.4592	−4.4577
RMS	0.0037	0.0025	0.0278	0.0261
R	0.99997	0.99999	0.99989	0.99987
MAE (%)	0.1850	0.1218	0.5782	0.6692
Network testing				
Number of testing patterns	129	129	129	129
Maximum error (%)	0.9761	6.7819	3.5241	3.9416
Minimum error (%)	−1.1407	−0.8680	−5.1794	−4.8844
RMS	0.0044	0.0089	0.0412	0.0504
R	0.99995	0.99980	0.99957	0.99947
MAE (%)	0.2344	0.3711	0.7914	1.1252

plate shape factors for membrane and bending stress obtained from Newman–Raju equations.

Two hundred and seventy patterns are chosen for training and the rest (129 patterns) for testing the networks in a similar manner for four *Mk* factors. The patterns which include the maximum and minimum values are placed in training set and subsequently the *Mk* values are normalized between 0.0 and 1.0. MLP networks with logistic sigmoid transfer function in all neurons are selected for network's architecture. The training algorithm is *Back Propagation* for all networks. Best configurations of networks for each *Mk* are obtained by trial and error process. Several MLP networks with different numbers of hidden layers, numbers of neurons in each layer and numbers of training cycles are designed, trained and tested. To evaluate the efficiency of each trained network, five error criteria, i.e. RMS, MAE, *R*, *Maximum error* and *Minimum error* for each network in both training and testing sets are calculated and the best networks with lower level of errors are selected. Table 4 shows the characteristics of neural networks with optimum capability in prediction *of* Mk_{ma}, Mk_{ba}, Mk_{mc} and Mk_{bc}.

4.3. Validation

Figs. 11–14 show the *Mk* factors obtained from Finite Element (FE) modeling, versus predicted values for training and testing data sets and the related *trendlines*. These lines should be $(y = x)$ in ideal case of prediction. These figures show that the predicted values by networks are very close to Finite Element based values. In the test set, the

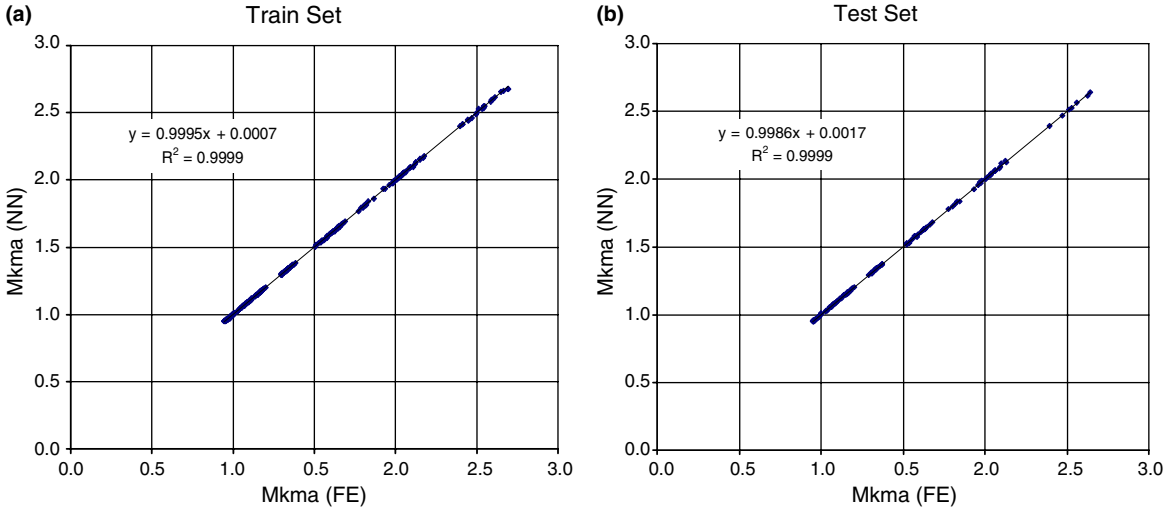

Fig. 11. Predicted Mk_{ma} versus Finite Element based values – train and test sets.

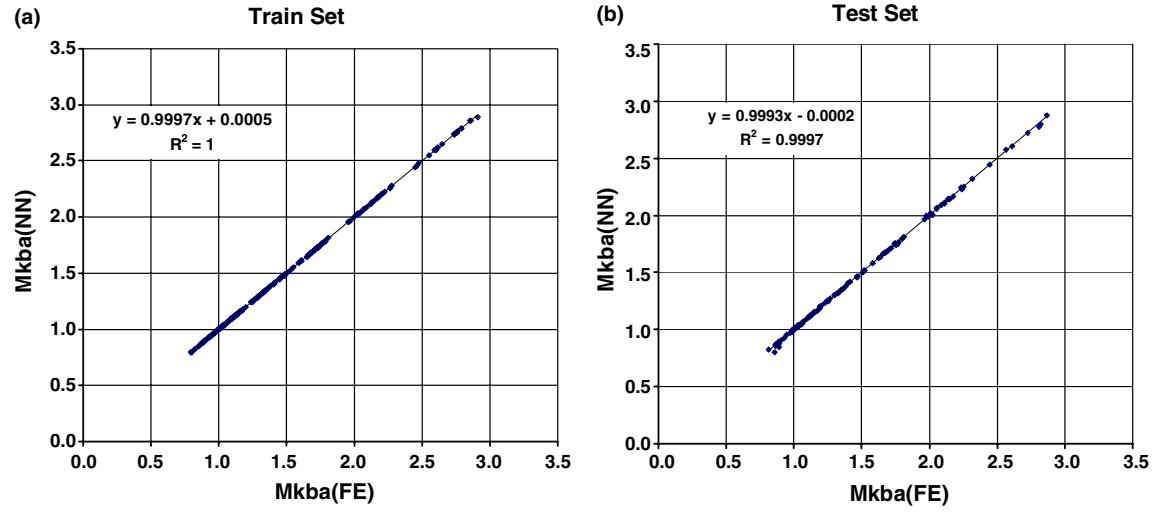

Fig. 12. Predicted Mk_{ba} versus Finite Element based values – train and test sets.

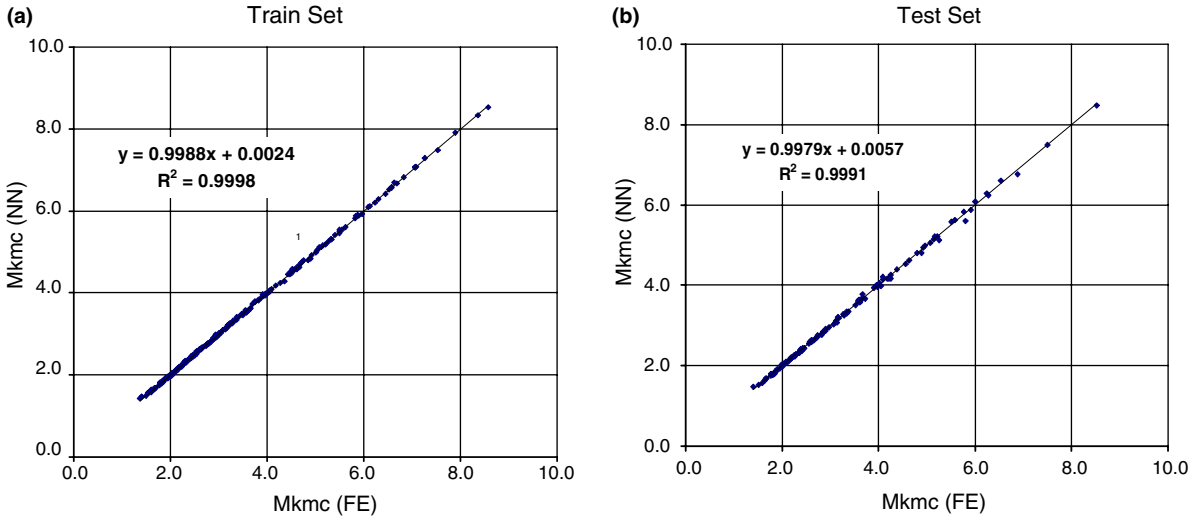

Fig. 13. Predicted Mk_{mc} versus Finite Element based values – train and test sets.

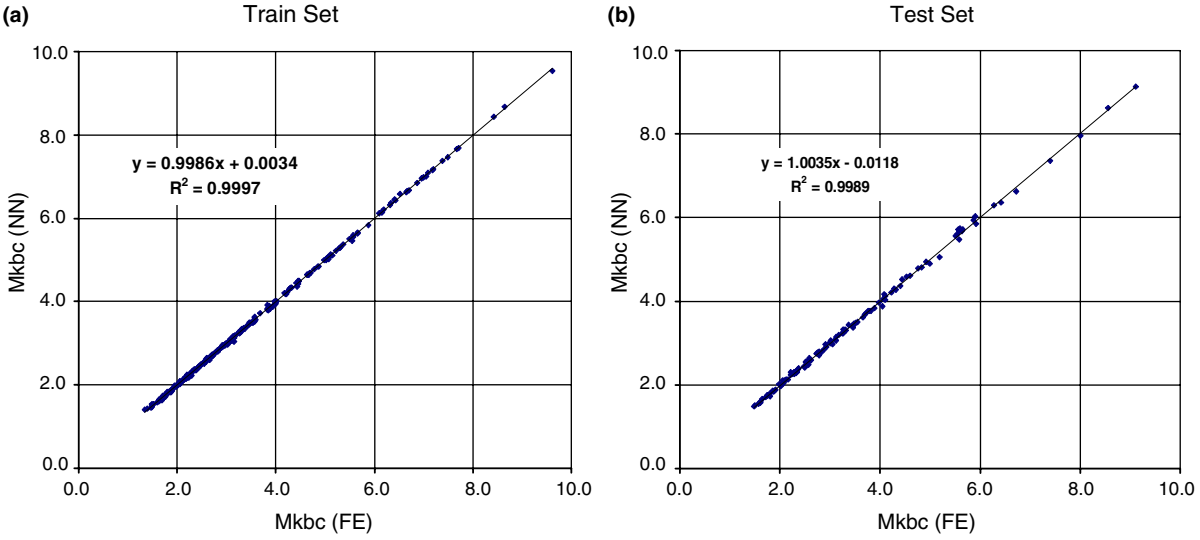

Fig. 14. Predicted Mk_{bc} versus Finite Element based values – train and test sets..

agreement between predicted *Mk* and Finite Element based values is particularly encouraging, considering the fact that the networks never receive any information about test set during training process. The results of networks are also compared with Lee and Bowness equations. Fig. 15 shows the frequency of error for both methods in training and testing sets. These figures illustrate that the networks can predict *Mk* factors better than parametric equation even in testing sets.

5. Prediction of the fatigue life of tubular joints using NN

In this section, the networks developed in previous sections are used to predict fatigue lives of tubular joints. This method is used to predict the fatigue lives of 16_{mm} tubular T-joints under axial loading from the HSE database [23]. Table 5 shows the geometrical parameters and stress condition of each joint. The basic procedure for performing crack growth calculations is presented in Fig. 16. The procedure contains two major parts:

- Part one ($0.0 < a/T < 0.2$)
  Fatigue life calculations are based on T-butt solutions in this part. For each crack, *Mk* factors are calculated by MLP neural networks developed in Section 4. Shape factors are calculated using Newman–Raju equations. The crack growth in width and depth direction is calculated using Paris crack growth law. Key input data for networks in this part are a/T, a/c, θ and L/T.
- Part two ($0.02 < a/T < 1.0$)
  In this part the weld geometry effects on crack growth are neglected. The RBF network developed in Section 3

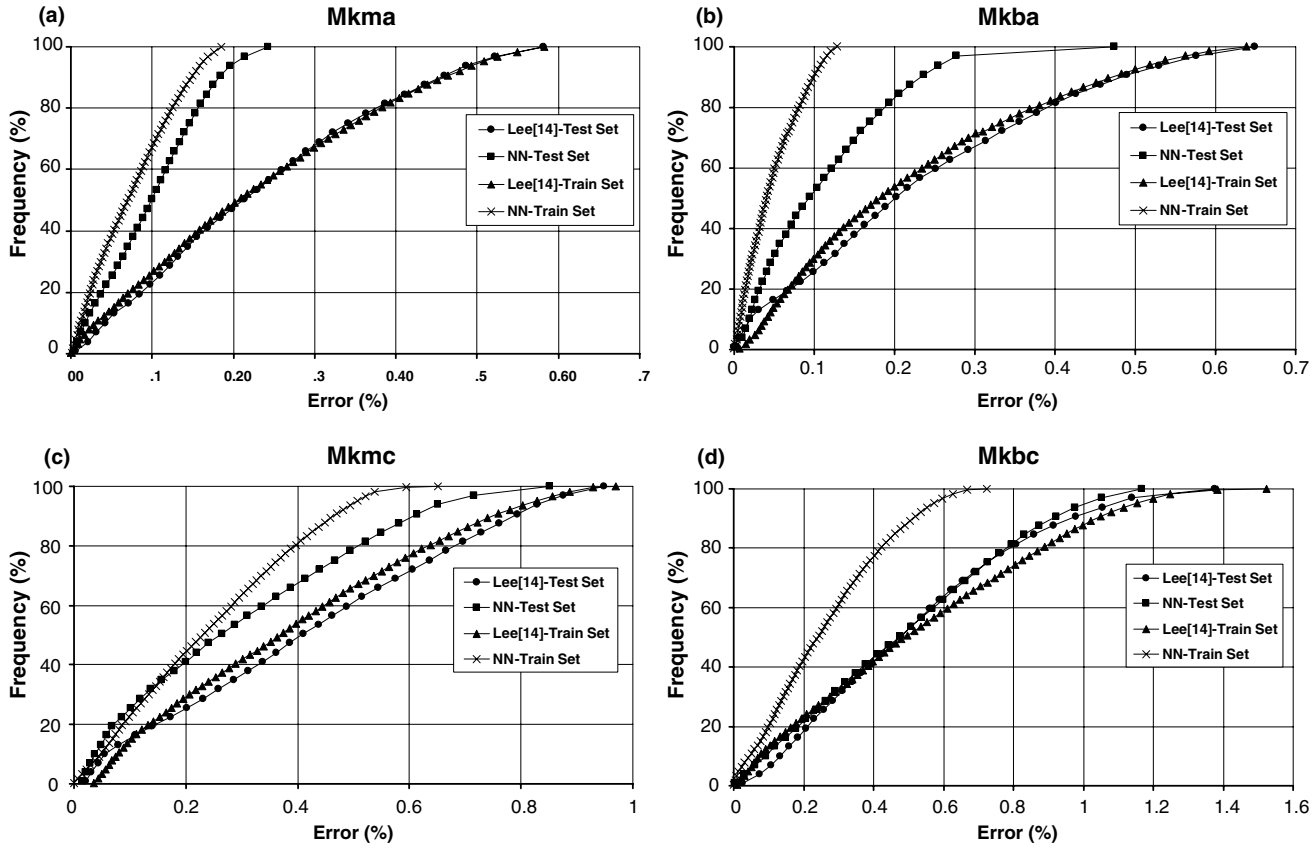

Fig. 15. Frequency of error for NN and Lee–Bowness method in predicting *Mk* factors.

Table 5
Tubular T-joints from the HSE 16 mm tubular joints fatigue database used in fatigue life calculations

Specimen number	98	100	104	112	113	116	190	191	192	193	194	195	196
Joint type	T	T	T	T	T	T	T	T	T	T	T	T	T
D (mm)	457	457	457	457	457	457	457	457	457	457	457	457	457
T (mm)	15.7	15.8	16.1	16.4	16.4	16.3	16	16	16	16	16	16	16
α	10.2	10.2	10.2	10.2	10.2	10.2	8.8	8.8	8.8	8.8	8.8	8.9	8.9
β	1	1	1	1	1	1	0.5	0.5	0.5	0.5	0.5	0.2	0.2
γ	14.6	14.5	14.2	13.9	13.9	14	14.3	14.3	14.3	14.3	14.3	14.3	14.3
τ	1.1	1.1	1.1	0.6	0.6	0.6	0.5	0.5	0.5	0.5	0.5	0.4	0.4
DOB	0.803	0.801	0.798	0.682	0.682	0.683	0.818	0.818	0.818	0.818	0.818	0.799	0.799
Loading mode	AX	AX	AX	AX	AX	AX	AX	AX	AX	AX	AX	AX	AX
$(\Delta\sigma_{min}/\Delta\sigma_{max})$	−1	−1	−1	−1	−1	−1	0	0	0	0	0	−1	−1
$\Delta\sigma_{HS}$	322	190	120	204	146	269	198	179	179	105	198	123	242
N (10^3)	144	1000	6950	535	1980	369	680	1000	840	7500	760	9000	700
Intersection location	1.57	1.57	1.57	1.57	1.57	1.57	1.57	1.57	1.57	1.57	1.57	1.57	1.57
Local dihedral angle, Ψ	180	180	180	180	180	180	120	120	120	120	120	102	102
L (mm)	30.2	30.4	31	17.2	17.2	17.1	10.8	10.8	10.8	10.8	10.8	9	9
L/T	1.93	1.93	1.93	1.05	1.05	1.05	0.67	0.67	0.67	0.67	0.67	0.56	0.56
Θ used	30	30	30	30	30	30	60	60	60	60	60	70	70

is used to predict Y factor in deepest point of crack. Key input data for this part are a/T and a/c. The designed RBF network which is able to predict Y factor in tubular T-joints, is not sensitive to geometrical parameters of tubular joints because the data used for training RBF network were from six similar joints. Therefore the Y factor predicted by RBF network is modified using AVS model [14] to consider the geometrical effects of tubular joints through the following equation:

$$Y_{1(\mathrm{HSE})} = \frac{Y_{\mathrm{AVS(HSE)}}}{Y_{\mathrm{AVS(NDE)}}} \times Y_{0(\mathrm{HSE})} \tag{13}$$

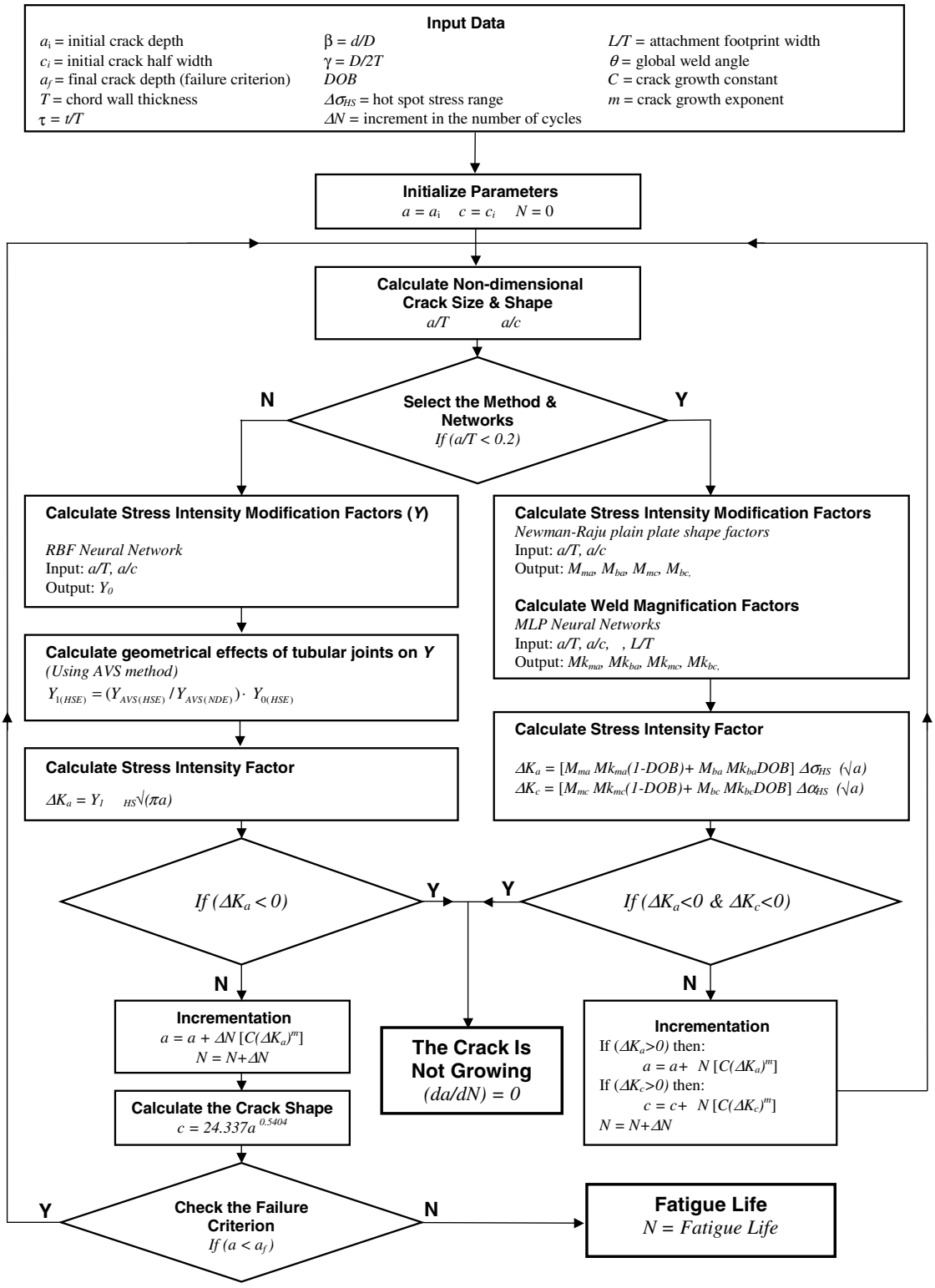

Fig. 16. Basic flowchart for crack growth calculation.

where $Y_{1(\mathrm{HSE})}$ is the modified Y factor to be used in Paris law, $Y_{\mathrm{AVS(HSE)}}$ the Y factor of HSE joints calculated by AVS method, $Y_{\mathrm{AVS(NDE)}}$ the Y factor of the joint with geometrical parameters the same as the ones used to train the RBF network and having a crack similar to that of the HSE joint and $Y_{0(\mathrm{HSE})}$ is the Y factor of HSE joints estimated by RBF network.

An exponential equation obtained by curve fitting on the crack shapes data of six *NDE* experiments, is used to predict a/c for the cracks. This equation is:

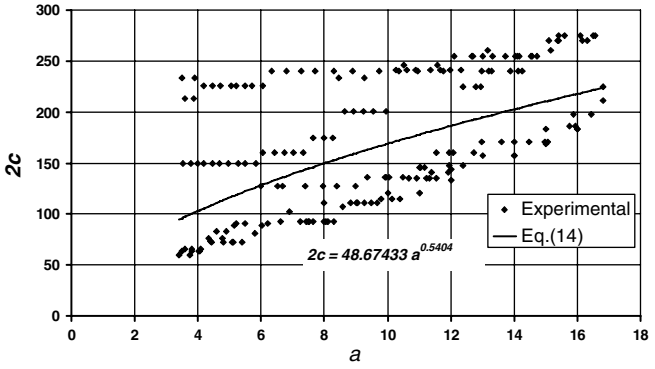

Fig. 17. Experimental crack shape and prediction curve.

$$2c = 48.674a^{0.5404} \tag{14}$$

Fig. 17 shows the crack aspect ratio and the fitted curve in six T-joints. The exponential pattern of crack shape development is previously used by Etube [18] and Myers [6] for Y and T-joint, respectively.

The following assumptions were considered for fatigue life calculations. They are almost similar to what Lee and Bowness [22] assumed for their calculation.

- The Paris crack growth constants were taken to be $C = 1.8318 \times 10^{-13}$ and $m = 3.0$ (mean values for steel in air [23].
- The *entire* range of the hot spot stress is considered to be damaging.
- *The* hot spot stress field of uncracked joint is applied to the deepest point and crack ends.
- A single crack is assumed to exist with initial values $a_i = c_i = 0.25_{\text{mm}}$ which is the typical slag intrusion at the weld toe.
- The number of cycles is incremented by 10.
- Failure is deemed to have occurred when crack grows through the chord wall thickness i.e. $a_f = T$.

Table 6 shows the result of fatigue crack calculation using NN.

6. Conclusion

As assessing fatigue cracks in tubular joints is a very complicated subject due to geometrical complexity of tubular joints, NN provides the possibility to directly use the existing experimental fatigue data of tubular joints to predict crack growth rates and fatigue lives. A well trained set of networks is expected to be helpful as a computational tool for the prediction of fatigue crack growth rate in tubular joints The solution procedure and subsequently the result of prediction by means of NN are highly dependent on the quality and quantity of training database. The network and procedure used in this research could provide more accurate results if the training data base were more comprehensive or if they could be enhanced by more experimental data.

Table 6
Results of fatigue life calculations

Specimen number	98	100	104	112	113	116	190	191	192	193	194	195	196
N	144,000	1,000,000	6,950,000	535,000	1,980,000	369,000	680,000	1,000,000	840,000	7,500,000	760,000	9,000,000	700,000
HSE mean 16_{mm} S–N curves	262,000	1,276,000	5,064,000	1,031,000	2,812,000	450,000	1,127,000	1,526,000	1,526,000	7,558,000	1,127,000	4,702,000	617,000
NN based method	327,000	1,424,010	656,4350	790,260	1,992,980	572,220	1,010,430	1,140,360	1,140,360	14,166,200	1,010,430	12,870,750	482,530
Prediction/N	2.271	1.424	0.945	1.477	1.007	1.551	1.486	1.140	1.358	1.889	1.330	1.430	0.689

Acknowledgements

The authors gratefully acknowledge help and support from Professor W.D. Dover, Dr. F. Brennan and Dr. Bijan Talie-Faz from NDE center of University College London, for providing experimental crack growth data.

References

[1] Etube LS. Fatigue and fracture mechanics of offshore structures. London: Professional Engineering Publishing; 2001.
[2] Newman JC, Raju IS. An empirical stress intensity factor equation for the surface cracks. Eng Fract Mech 1981;12(2):185–92.
[3] Fauset L. Fundamentals of neural networks, architectures, algorithms and applications. New Jersey: Prentice-Hall International Inc.; 1994.
[4] Sarimveis H, Doganis P, Alexandridis A. A classification technique based on radial basis function neural networks. Adv Eng Software 2006;37:218–21.
[5] Shi D, Yeung DS, Gao J. Sensitivity analysis applied to the construction of radial basis function networks. Neural Networks 2005;18:951–7.
[6] Myers P. Corrosion fatigue fracture mechanics of high strength jack-up steels. PhD thesis submitted to London University; February 1998.
[7] Talie-faz B, Dover WD, Brenan FP. Static strength of cracked high strength tubular joints. London: Health and Safety Executive (HSE); 2002.
[8] Iacoviello F, Iacoviello D, Cavallini M. Analysis of stress ratio effects on fatigue propagation in a sintered duplex steel by experimentation and artificial neural network approaches. Int J Fatigue 2004;26: 819–28.
[9] Genel K. Application of artificial neural network for predicting strain-life fatigue properties of steels on the basis of tensile tests. Int J Fatigue 2004;26:1027–35.
[10] Kang Jae-Youn, Choi Byung-Ik, Lee Hak-Joo, Kim Joo-Sung, Kim Kee-Joo. Neural network application in fatigue damage analysis under multiaxial random loadings. Int J Fatigue 2006;28:132–40.
[11] Marquardt C, Zenner H. Lifetime calculation under variable amplitude loading with the application of artificial neural networks. Int J Fatigue 2005;27:920–7.
[12] Harpham C, Dawson CW. The effect of different basis functions on a radial basis function network for time series prediction: a comparative study. Neurocomputing 2005.
[13] Akhlaghi Y, Kompany-Zareh M. Comparing radial basis function and feed-forward neural networks assisted by linear discriminant or principal component analysis for simultaneous spectrophotometric quantification of mercury and copper. Anal Chim Acta 2005;537: 331–8.
[14] Dover WD, Darmavasan S. Fatigue fracture mechanics analysis of T and Y joints. Paper OTC 4404 of Offshore Technology Conference, TX 1982.
[15] Austin JA. The role of corrosion fatigue crack growth mechanics in predicting fatigue life of offshore tubular joints. PhD thesis, Department of Mechanical Engineering, University College London; October 1994.
[16] Kam JC. Structural integrity of offshore tubular joints subjected to fatigue. PhD thesis, Department of Mechanical Engineering, University College London; July 1989.
[17] Aghakouchak AA, Glinka G, Dharmavasan S. A load shedding model for fracture mechanics analysis of fatigue cracks in tubular joints. In: Offshore mechanics and arctic engineering conference (OMAE); 1989. p. 159–65.
[18] Etube LS, Brenan FP, Dover WD. A new method for predicting stress intensity factor in cracked welded tubular joints. Int J Fatigue 2000;22:447–56.
[19] Monahan CC. Early fatigue crack growth in offshore structure. PhD thesis, Department of Mechanical Engineering, University College London; May 1994.
[20] Cheaitant MJ, Bolt HM. Evaluation of stress intensity factor solutions for offshore tubular joints. In: Offshore mechanics and arctic engineering conference (OMAE); 1996. p. 521–32.
[21] Bowness D, Lee MMK. Prediction of Weld toe magnification factors for semi-elliptical cracks in t-butt joints. Int J Fatigue 2000;22: 369–87.
[22] Lee MMK, Bowness D. Fracture mechanic assessment of fatigue cracks in offshore tubular structures. London: Health and Safety Executive; 2000.
[23] HSE 1995. Background to new fatigue guidance for steel joints and connections in offshore structures. Health and safety Executive, O/S Technical Report OTH 92 390.